Design and Operation of Blind Interference Alignment in Cellular and Cluster-Based Systems

Chenwei Wang*, Haralabos C. Papadopoulos†, Sean A. Ramprashad† and Giuseppe Caire‡
* EECS Dept., University of California, Irvine, Irvine, CA 92697
† DoCoMo Communications Labs USA, Inc., Palo Alto, CA 94304
‡ EE Dept., University of Southern California, Los Angeles, CA 90089

***Abstract*—We consider the use of Blind Interference Alignment (BIA) in a cellular environment as a means for supporting downlink Multi-User MIMO (MU-MIMO) transmission without the need for channel state information at the transmitter (CSIT). This "CSIT-blind" characteristic of BIA is of particular interest for Frequency Division Duplex (FDD) systems, since it allows one to eliminate overheads and impairments due to downlink pilot training and CSIT quantization and feedback. As we demonstrate, when properly applied over cellular, BIA can enable control of both intra-cell and inter-cell interference. In this context, we explore the aspects of power-allocation, frequency reuse, and alignment-code reuse and their effect on cellular performance. BIA can also be jointly applied over clusters of cells. Cluster operation leads to lower inter-cell interference levels and potentially improved BIA system performance. BIA however, has some interesting operational aspects when used with clusters. These include some benefits over CSIT-based MU-MIMO since individual cells do not need to share channel knowledge and can transmit independent information streams, some challenges in more complex receiver hardware, and relationships to cellular with code-reuse. We discuss such aspects and investigate the application of BIA in both cellular and cluster deployments.**

I. Introduction

Multiple Input Multiple Output (MIMO) techniques can be used in wireless systems to increase spectral efficiency and/or provide additional diversity. They do so effectively by the increasing in the number of "Degrees of Freedom" (DoFs) available for transmission. For the downlink, the maximum number of DoFs possible in both Single-User MIMO (SU-MIMO) and Multi-user MIMO (MU-MIMO) systems is $\min(N_t, KN_r)$, where N_t is the number of transmit antennas serving K users each with N_r antennas. This motivates systems with increased N_t and N_r, and even increased K.

Achieving such DoFs, however, often requires some knowledge of Channel State Information (CSI) between the transmit and receive antennas. We refer to CSI available the transmitter as CSIT, and CSI available to the receiver as CSIR. For traditional MU-MIMO systems, such as Linear Zero Forced Beamforming (LZFB), CSIT is essential. Unfortunately in Frequency Division Duplex (FDD) systems this becomes an issue since CSIT mandates use of wireless resources for CSI-estimation pilots and CSI feedback [1]. CSIT thus results in both overheads and challenges in obtaining accurate CSI, and this can limit the growth in spectral efficiency (with increased N_t,N_r and K) for CSIT-based MU-MIMO [2]. MU-MIMO systems that can operate without CSIT are therefore of interest.

Recently a class of "Blind Interference Alignment" (BIA) MU-MIMO techniques has demonstrated such a possibility [3]. The schemes leverage multiple, e.g. M different, reconfigurable antenna modes at each receiver. By using the codes in [3], and predermined antenna-switching patterns at each receiver, the system can create multiple concurrent non-interfering transmissions with DoF benefits, much like CSIT-based MU-MIMO. The value M is yet another design parameter along with N_t, N_r and K. While attractive in removing dependencies on CSIT, BIA has inherent challenges and operational aspects that must be considered carefully in a cellular setting. For example, the ZF process amplifies noise at the receiver, thus requiring high SNR or Signal to Interference plus Noise Ratio (SINR) to operate effectively [3]. In addition, the technique does require CSIR and so it is not completely "blind" in its CSI requirements [5]. Furthermore, the deployment/operation of codes between cells, or in clusters of cells, have both benefits and challenges compared to CSIT-based MU-MIMO.

In this paper we consider a number of these issues. We begin by studying the effect of noise amplification due to ZF interference, and the benefit of optimizing the power allocation in the BIA code structure to minimize this effect. We then study the BIA performance in a two-cell model, considering isotropic interference, as well as interference from BIA transmission with aligned and misaligned code structures.

We then consider operational and performance aspects of BIA MU-MIMO in more complete cellular and cluster-based transmission. Motivated by the two-cell example, we focus on the use of aligned BIA code structures throughout the cellular topology. We consider conventional and BIA-specific operational aspects, and evaluate the ergodic rates provided by aligned BIA schemes with conventional cellular and cluster transmission, using both traditional frequency reuse as well as BIA code-reuse. In the process, we also highlight some of the operational advantages of BIA MU-MIMO with respect to conventional MU-MIMO and Network MIMO [4], including eliminating the need for joint processing across cells in cluster-based transmission, and the ability of removing a significant portion of ICI without CSIT. The paper complements the work in [5] which considers issues of CSIT and CSIR overheads and comparisons to LZFB, to give a broader picture on the use of BIA in cellular deployments.

II. BIA DL MU-MIMO

In this section we first review the BIA MU-MIMO scheme proposed in [3], and then explore power-allocation variations

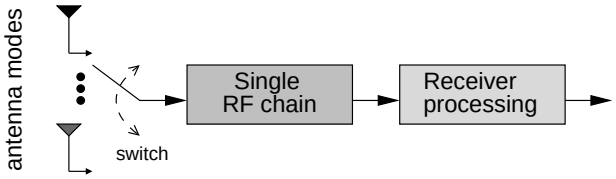

Fig. 1. Illustration of a multi-mode antenna receiver.

with improved performance characteristics. Consider a K user $M\times 1$ Multiple Input Single Output Broadcast Channel (MISO BC), where the transmitter has $N_t = M$ antennas. Each receiver is equipped with one reconfigurable antenna (and thus only one RF chain) as shown in Figure 1 that can switch among M preset modes, each of which is able to see a channel that is linearly independent of the channel of other modes. Let K denote the number of such multi-mode antenna receivers (users) that are simultaneously served in the downlink by the N_t transmit antennas. We use the notation $\mathbf{h}^{[k]}(m) \in \mathbb{C}^{1\times N_t}$ to denote the channel vector associated with the mth antenna mode at the receiver where $k \in \{1,\ldots,K\}$ and $m \in \{1,\ldots,M\}$, and define

$$\mathbf{H}^{[k]} = \left[\mathbf{h}^{[k]^\mathsf{T}}(1) \quad \mathbf{h}^{[k]^\mathsf{T}}(2) \quad \cdots \quad \mathbf{h}^{[k]^\mathsf{T}}(M)\right]^\mathsf{T}. \tag{1}$$

We consider a specific illustrative example which helps in understanding the general BIA approach. In particular, we denote a BIA scheme by the pair "(M,K)", and will present the original BIA scheme from [3] where ($M = 2$, $K \geq 2$) case, i.e., the case of $M = 2$ transmit antennas and receive antenna modes and $K \geq 2$ users.

The scheme achieves the optimal $MK/(M+K-1) = 2K/(K+1)$ DoFs in the absence of CSIT [3, Theorem 1] by sending two scalar symbols to each user via a $(K+1)$-slot strategy. This strategy relies on jointly coordinated transmission and antenna-mode switching. Let $\mathbf{u}^{[k]} = [u_1^{[k]}\ u_2^{[k]}]^\mathsf{T}$ with $u_i^{[k]}$ denoting the ith data stream of user k. Letting $\mathbf{x}(n)$ denote the nth transmitted (two-dimensional) symbol. A total of $K+1$ slots are used to transmit $K+1$ two-dimensional symbols where [3]

$$\mathbf{x}(1) = \textstyle\sum_{k=1}^{K}\mathbf{u}^{[k]} \qquad \text{(first slot)} \tag{2a}$$
$$\mathbf{x}(n) = \mathbf{u}^{[n-1]} \qquad \text{for } 2 \leq n \leq K+1\ . \tag{2b}$$

User k cycles a antenna switching pattern that is user specific to enable blind interference alignment of the interfering streams. In particular user k uses antenna mode 1 on all slots except in slot $n = k+1$. Letting $y^{[k]}(n)$ denote the received signal sample of user k in slot n, for $n \neq k+1$ we have

$$y^{[k]}(n) = \mathbf{h}^{[k]}(1)\mathbf{x}(n) + z^{[k]}(n) \tag{3a}$$

while

$$y^{[k]}(k+1) = \mathbf{h}^{[k]}(2)\mathbf{x}(k+1) + z^{[k]}(k+1) \tag{3b}$$

and where $\mathbf{z}^{[k]} = [z^{[k]}(1)\ z^{[k]}(2)\ \cdots\ z^{[k]}(K+1)] \sim \mathcal{CN}(\mathbf{0},\mathbf{I})$. For each user k, the interference from other users' streams (in $y^{[k]}(1)$) can be then canceled out by taking a linear combination of the K measurements from set (3a); letting

$$\tilde{\mathbf{y}}^{[k]} = \begin{bmatrix}\tilde{y}^{[k]}(1)\\ \tilde{y}^{[k]}(2)\end{bmatrix} = \begin{bmatrix} y^{[k]}(1) - \sum_{n\neq 1,k+1} y^{[k]}(n)\\ y^{[k]}(k+1)\end{bmatrix} \tag{4}$$

and using (2) and (3) we have

$$\tilde{\mathbf{y}}^{[k]} = \mathbf{H}^{[k]}\mathbf{u}^{[k]} + \tilde{\mathbf{z}}^{[k]} \tag{5}$$

where $\mathbf{H}^{[k]}$ is given by (1), and $\tilde{\mathbf{z}}^{[k]} \sim \mathcal{CN}(\mathbf{0},\mathbf{R}_{\tilde{\mathbf{z}}})$, with $\mathbf{R}_{\tilde{\mathbf{z}}} = \mathrm{diag}(K,1)$.

In the general case, involving $N_t = M$ transmit antennas (and M receive antenna modes) and K users, a total of $N = (M-1)^{K-1}$ M-dimensional symbols are sent to each of the K users with a single BIA code of length $N(M+K-1)$ [3]. In the nomenclature of [3], $N(M-1)$ of the slots comprise "*alignment block 1*". Each of these slots is a linear combination of K symbols, one per user, much like slot 1 of the $M = 2$ code in (2a). The remaining KN slots, comprising "*alignment block 2*", are employed to transmit one of each of the N different M-dimensional symbols of each user, one at a time, similar to the transmissions in (2b). By carefully coordinating the linear combinations transmitted in alignment block 1 with each user's antenna mode switching patterns, and by user-specific post processing to zero-force interference, each user is able to pick out its own N M-dimensional symbols free from other user interference. The process of zero-force interference is very similar to the $M = 2$ case described earlier. Here, instead of going too much details of constructing alignment block, we show an intuition of that process as follows. To pick out a given symbol user k uses

(a) $(M-1)$ received samples from alignment block 1; the ith such sample contains the user's desired symbol in a different linear combination with other users' symbols; the ith of these samples is seen by the ith antenna mode.
(b) For each $i \in \{1,2,\cdots,M-1\}$, $(K-1)$ received samples from alignment block 2 are used to remove interference from the ith sample from (a). The user uses the ith antenna mode for all these slots.
(c) One extra sample from alignment block 2 is used, containing the user's desired symbol seen by the user through its Mth antenna mode.

By following a zero-forcing (ZF) cancellation analogous to the $M = 2$ case, user k obtains a processed (M-dimensional) vector of the form (5), where $\tilde{\mathbf{y}}^{[k]}$, $\tilde{\mathbf{z}}^{[k]}$ and $\mathbf{u}^{[k]}$ are all $M\times 1$ vectors, and $\tilde{\mathbf{z}}^{[k]} \sim \mathcal{CN}(\mathbf{0},\mathbf{R}_{\tilde{\mathbf{z}}})$, with

$$\mathbf{R}_{\tilde{\mathbf{z}}} = \begin{bmatrix} K\mathbf{I}_{M-1} & \mathbf{0}\\ \mathbf{0} & 1\end{bmatrix}. \tag{6}$$

For the sake of the terminology of this paper, we restate [3, Theorem 1]:

Theorem 1: [3] For the K user $M\times 1$ MISO BC, a total of $\frac{MK}{M+K-1}$ DoF can be achievable, almost surely.

A. Optimizing Power Allocation to two Alignment Sub-blocks

Although the scheme shown in (2) and its generalizations [3] achieves the maximum DoF, its low SNR performance is

far from optimal as it suffers from noise amplification due to the ZF interference step. In fact, even at high SNR its performance can also be improved. In particular, by varying the relative transmit power allocated to symbols in alignment block 1 and alignment block 2 slots, power-optimized schemes can be designed that outperform the original BIA schemes.

In the original BIA every transmitted symbol is transmitted at the same power level in both types of alignment blocks. In the power optimized schemes the power allocated to each symbol is changed as a function of the alignment block type. We use δ to denote the ratio of the power used for transmitting a user symbol in alignment block 1 over the corresponding power in alignment block 2. The power ratio δ can be chosen to control the noise enhancement levels and improve the effective SU-MIMO channel obtained after zero-forcing interference.

In the $(M = 2,\ K \geq 2)$ case, $K+1$ slots are used to transmit $K+1$ two-dimensional symbols. In this case the nth transmitted vector symbol $\mathbf{x}(n)$ is given by[1]

$$\mathbf{x}(1) = \sqrt{\delta}\sum_{k=1}^{K}\mathbf{u}^{[k]} \quad \text{(slot one)} \tag{7a}$$

$$\mathbf{x}(n) = \mathbf{u}^{[n-1]} \quad \text{for } 2 \leq n \leq K+1\ . \tag{7b}$$

The two receiver modes at receiver k are cycled through the same user-specific way as with the original scheme to enable blind interference alignment of the interfering streams. In particular user k uses mode 1 on all slots except slot $n = k+1$ and obtains a set of measurements of the form (3). The interference from other user streams (in $y^{[k]}(1)$) can be then canceled out by taking a linear combination of the K measurements in the measurement set (3a). This linear combination is δ-value specific, *viz.*,

$$\tilde{\mathbf{y}}^{[k]} = \begin{bmatrix}\tilde{y}^{[k]}(1)\\ \tilde{y}^{[k]}(2)\end{bmatrix} = \begin{bmatrix}(1/\sqrt{\delta})y^{[k]}(1) - \sum_{n\neq 1,k+1} y^{[k]}(n)\\ y^{[k]}(k+1)\end{bmatrix}\ . \tag{8}$$

Using (7) and (3), we can express (8) in the form (5) with $\tilde{\mathbf{z}}^{[k]} \sim \mathcal{CN}(\mathbf{0}, \mathbf{R}_{\tilde{\mathbf{z}}})$, and $\mathbf{R}_{\tilde{\mathbf{z}}} = \mathrm{diag}(\delta^{-1}+K-1, 1)$.

In the general $(M,\ K)$ case, after ZF cancellation each user has an effective SU-MIMO channel of the form (5) with

$$\mathbf{R}_{\tilde{\mathbf{z}}} = \begin{bmatrix}(\delta^{-1}+K-1)\,\mathbf{I}_{M-1} & \mathbf{0}\\ \mathbf{0} & 1\end{bmatrix}. \tag{9}$$

As a result, we have the following:

Theorem 2 For the K user $M\times 1$ MISO BC, the achievable sum rate zero-forcing interference at each user is given by

$$R = \sum_{k=1}^{K}\frac{1}{M+K-1}\mathbb{E}\log\left|\mathbf{I} + \tilde{p}\mathbf{H}^{[k]}\mathbf{H}^{[k]^{\mathsf{H}}}\mathbf{R}_{\tilde{\mathbf{z}}}^{-1}\right| \tag{10}$$

where $\tilde{p} = \frac{(M+K-1)P}{MK((M-1)\delta+1)}$ and $\mathbf{R}_{\tilde{\mathbf{z}}}$ is given by (9).

Proof: Omitted due to the space limitations.

[1]Note the symbols $\{\mathbf{u}^{[n]}\}$ would have an overall scaling which depends on δ so that the average transmit energy in (7) is the same as in (2). For simplicity we suppress this dependence in notation, and compare different schemes at the same average transmit energy, i.e. same SNR.

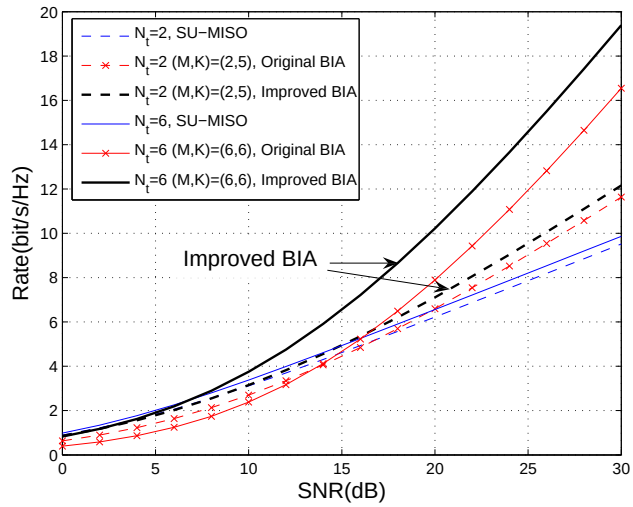

Fig. 2. Rate Comparison in the Low SNR Regime

B. The Constant Transmit-Power Scheme

The choice $\delta = 1/K$ in (7) is of interest since it leads to a constant-power scheme, hence avoiding power fluctuation in the time domain. In that case the effective SU-MIMO channel on any symbol transmitted to the kth user is given by (5) with

$$\mathbf{R}_{\tilde{\mathbf{z}}} = \begin{bmatrix}(2K-1)\,\mathbf{I}_{M-1} & \mathbf{0}\\ \mathbf{0} & 1\end{bmatrix}. \tag{11}$$

The sum-rate provided by the constant-power scheme is given by (10) for $\delta = 1/K$, which reduces to

$$R = \sum_{k=1}^{K}\frac{1}{M+K-1}\mathbb{E}\log\left|\mathbf{I} + \frac{P}{M}\mathbf{H}^{[k]}\mathbf{H}^{[k]^{\mathsf{H}}}\mathbf{R}_{\tilde{\mathbf{z}}}^{-1}\right| \tag{12}$$

with $\mathbf{R}_{\tilde{\mathbf{z}}}$ given by (11).

C. Performance of the Schemes of Varying Power Allocation

We next consider the benefits of power optimized BIA schemes, focusing in particular to the benefits of the constant-power scheme ($\delta = 1/K$). As shown in Fig. 2, the constant-power BIA scheme (labeled "Improved BIA" on the figure) has reduced noise enhancement characteristics with respect to the original BIA scheme. And as Fig. 2 suggests, such constant-power BIA schemes are superior in performance to the original BIA scheme, with benefits increasing with larger N_t and K. Specifically, the cross point moves from around 17 dB to 10 dB for $N_t = 2,\ K = 5$. For $N_t = K = 6$, the cross point moves from around 16 dB to 7 dB. Here, also, the rate loss is negligible even at low SNR with the improved BIA performing better than SU-MISO in nearly all SNR regimes.

D. High-SNR Optimal Power Allocation in BIA Schemes

In principle, the value of power ratio, δ, can be chosen to maximize the ergodic rate (10), as a function of M, K, and SNR (denoted by P). Rather than considering the rate (10) as a function of δ directly, we investigate the gap between the rate provide by the BIA scheme for arbitrary δ to the rate provided by the constant-power BIA scheme. From this we are

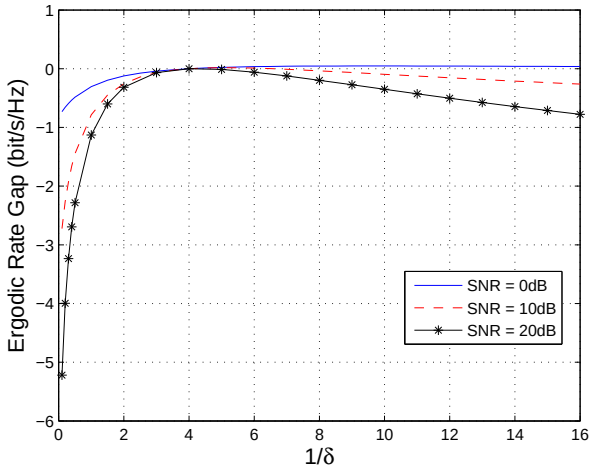

Fig. 3. Rate Gap when $(M, K) = (4, 4)$

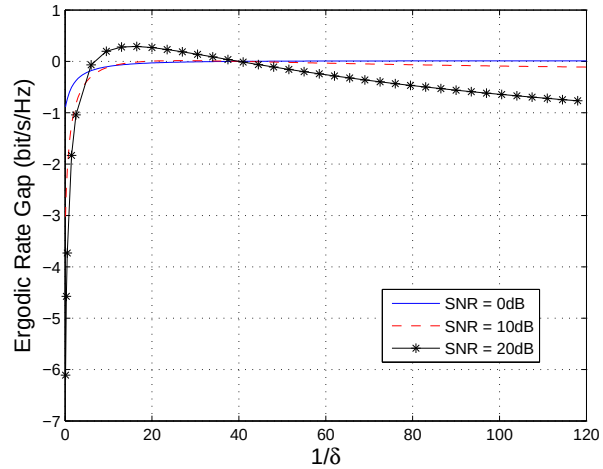

Fig. 4. Rate Gap when $(M, K) = (4, 40)$

able to see how much may be gained by further optimizing the power allocation ratio δ. We define a rate gap function:

$$\triangle R(P, \delta) = R_\delta(P) - R_{\delta=1/K}(P) \tag{13}$$

where $R_\delta(P)$ and $R_{\delta=1/K}(P)$ denote the rate given in Theorem 2 as a function of δ and for $\delta = 1/K$, respectively. We let $\delta_*(P)$ denote the value of δ that maximizes $\triangle R(P, \delta)$ in (13). In the limit of SNR $\to \infty$, (i.e., $P \to \infty$), we have:

$$\triangle R(\infty, \delta) = \tag{14}$$
$$\frac{KM}{M+K-1} \log\left[\frac{M+K-1}{K((M-1)\delta+1)}\right] - \frac{K(M-1)}{M+K-1} \log\left[\frac{K-1+\delta^{-1}}{2K-1}\right].$$

The value of δ_* that maximizes $\triangle R$ (can be readily found by finding the roots of the equation $\partial \triangle R(\infty, \delta)/\partial\delta = 0$) is given by

$$\delta_*(\infty) = \frac{2}{1+\sqrt{1+4M(K-1)}}. \tag{15}$$

The loss in performance of the constant-power scheme with respect to the δ optimized scheme (i.e., the BIA scheme $\delta = \delta_*$) is a function of M, K, and SNR. Consider first the case $M = K$. Substituting $M = K$ in (15) yields $\delta_*(\infty) = 1/K$, implying that when $M = K$, constant-power BIA maximizes the ergodic rate in the high SNR regime.

At finite SNR, the constant-power BIA scheme is not in general optimal. However, as Fig. 3 illustrates for the $(M, K) = (4, 4)$ case, and SNR $= 0,\ 10,\ 20$ dB, the rate loss of the constant-power scheme with respect to the optimal is negligible. In contrast, the rate loss of the original BIA scheme (case $\delta = 1$) can be significant.

Next we consider the case $K > M$. The high-SNR rate gap between the optimal and the constant-power scheme widens as K becomes large. In particular, for $M \ll K$, $\delta_*(\infty) \approx 1/\sqrt{MK}$, and $\triangle R(\infty, \delta_*) \approx M - 1$. This suggests that, in the high-SNR regime, it is possible to get a rate increase with respect to the constant-power scheme, which linearly depends on M. At the SNR levels of interest, in practice, however, the gains with respect to the constant-power scheme are negligible. Fig. 4 illustrates this point via $(M, K) = (4, 40)$ and SNR $= 0,\ 10$ and 20 dB. The above examples suggest that the constant-power scheme, i.e., the case with power allocation ratio $\delta = 1/K$, works uniformly well throughout the parameter space that is of interest in practice.

III. BIA DL MU-MIMO IN A TWO-CELL SETTING

As a prelude to using BIA in cellular transmission we consider the use of BIA in the presence of an interfering transmission. We again use the $(M = 2,\ K \geq 2)$ case as a driving example. We assume that in the cell of interest, $\mathbf{x}(n)$, of the form (7) for some δ, is transmitted over $K+1$ slots with goal to deliver streams $\mathbf{u}^{[1]}, \mathbf{u}^{[2]}, \cdots, \mathbf{u}^{[K]}$ to K users in the cell. In addition to thermal noise, the received signal of user k is corrupted by an interfering transmission captured by a random vector $\mathbf{x}_{\mathrm{I}}(n)$. In the context of two-cell setting for instance, this could represent the transmission from another base station. By following its antenna switching pattern (allowing user k to zero-force intra-cell interference), user k obtains the following measurements for $n \neq k+1$

$$y^{[k]}(n) = \mathbf{h}^{[k]}(1)\mathbf{x}(n) + \sqrt{\beta}\mathbf{h}_{\mathrm{I}}^{[k]}(1)\mathbf{x}_{\mathrm{I}}(n) + z^{[k]}(n) \tag{16a}$$

while for $n = k+1$

$$y^{[k]}(n) = \mathbf{h}^{[k]}(2)\mathbf{x}(n) + \sqrt{\beta}\mathbf{h}_{\mathrm{I}}^{[k]}(2)\mathbf{x}_{\mathrm{I}}(n) + z^{[k]}(n) \tag{16b}$$

where $\mathbf{z}^{[k]} = [z^{[k]}(1)\ z^{[k]}(2)\ \cdots\ z^{[k]}(K+1)]^{\mathsf{T}} \sim \mathcal{CN}(\mathbf{0}, \mathbf{I})$. Assuming equal average power in $\mathbf{x}(n)$ and $\mathbf{x}_{\mathrm{I}}(n)$, the quantity $-10\log_{10}\beta$ is a measure of the signal-to-interference ratio (SIR) in dB. We will consider the performance of the BIA scheme in the cell of interest, as a function of SNR and SIR for three different intercell interference (ICI) scenarios:

A: The interfering transmission $\mathbf{x}_{\mathrm{I}}(n)$ is a single BIA code, with the same M and K as $\mathbf{x}(n)$, that is synchronous and *aligned* in its structure with the $\mathbf{x}(n)$ transmission.

B: The interference $\mathbf{x}_{\mathrm{I}}(n)$ is a single BIA codeword transmission, synchronous and with the same M and K as $\mathbf{x}(n)$, but *not* aligned with the $\mathbf{x}(n)$ transmission.

C: The interference $\mathbf{x}_{\mathrm{I}}(n)$ comprises zero-mean i.i.d. vector samples, each with a scaled identity covariance.

In each case we derive expressions for the user achievable rates as a function of SNR and SIR.

A. Scenario A: Synchronous Aligned Code Reuse

Under Scenario A, the interference signal is an (M, K) BIA code, assumed to obey the same code structure as $\mathbf{x}(n)$. Focusing for illustration on the case $M = 2$, the interference signal $\mathbf{x}_{\rm I}(n)$ is given by (7) with $\mathbf{u}^{[k]}$ replaced by $\mathbf{u}_{\rm I}^{[k]}$. The vectors $\mathbf{u}_{\rm I}^{[k]}$ represent the information streams intended for the K users in the cell served by the interfering tower. Following the zero-forcing post-processing step (8) and assuming the receive model (16) yields at user k the following post-processed measurements

$$\tilde{\mathbf{y}}^{[k]} = \mathbf{H}^{[k]}\mathbf{u}^{[k]} + \sqrt{\beta}\mathbf{H}_{\rm I}^{[k]}\mathbf{u}_{\rm I}^{[k]} + \tilde{\mathbf{z}}^{[k]} \tag{17}$$

where $\tilde{\mathbf{z}}^{[k]} \sim \mathcal{CN}(\mathbf{0}, \mathbf{R}_{\tilde{\mathbf{z}}})$, with $\mathbf{R}_{\tilde{\mathbf{z}}}$ given by (9) and $\mathbf{H}_{\rm I}^{[k]}$ is defined analogously to $\mathbf{H}^{[k]}$ in (1). Note also that (17) applies in the general (M, K) case as presented in [3].

Comparison of (17) with (5) reveals that, from the point of view of the user using the kth BIA code in the cell of interest, intercell interference is experienced *only* from the kth coded stream of the BIA transmission of the interfering base station. Furthermore, observation of (17) suggests that, for a fixed SIR and SNR $\to \infty$, we get interference limited transmission and the effect of optimized power allocation of Section II (which affects the covariance $\mathbf{R}_{\tilde{\mathbf{z}}}$) becomes secondary.

Assuming the instantaneous covariance of the interference signal $\sqrt{\beta}\mathbf{H}_{\rm I}^{[k]}\mathbf{u}_{\rm I}^{[k]}$ is unknown to the kth receiver, the achievable ergodic sum-rate in the cell of interest is given by[2]:

$$R_{\rm A} = \tfrac{K}{M+K-1}\mathbb{E}\log\left|\mathbf{I} + \tilde{p}\mathbf{H}^{[k]}\mathbf{H}^{[k]\mathsf{H}}\left(\overline{\mathbf{R}}_{\mathbf{v},\rm A}\right)^{-1}\right| \tag{18}$$

where $\tilde{p} = \frac{(M+K-1)P}{MK((M-1)\delta+1)}$.

Here $\overline{\mathbf{R}}_{\mathbf{v},\rm A} = \mathbb{E}\left[\mathbf{R}_{\mathbf{v},\rm A}^{[k]}\right]$ and $\mathbf{R}_{\mathbf{v},\rm A}^{[k]}$ represents the covariance of the instantaneous aggregate interference experienced by the kth receiver after post-processing, i.e.,

$$\mathbf{R}_{\mathbf{v},\rm A}^{[k]} = \mathbf{R}_{\tilde{\mathbf{z}}} + \tilde{p}\beta\mathbf{H}_{\rm I}^{[k]}\mathbf{H}_{\rm I}^{[k]\mathsf{H}}. \tag{19}$$

Letting

$$\mathbf{R}_{\rm I,A}^{[k]} = \mathbf{H}_{\rm I}^{[k]}\mathbf{H}_{\rm I}^{[k]\mathsf{H}}, \tag{20}$$

we have

$$\overline{\mathbf{R}}_{\rm I,A}^{[k]} = \mathbb{E}\left[\mathbf{R}_{\rm I,A}^{[k]}\right] = M\mathbf{I}. \tag{21}$$

Thus (18) becomes

$$R_{\rm A} = \frac{K}{M+K-1}\mathbb{E}\log\left|\mathbf{I} + \tilde{p}\mathbf{H}^{[k]}\mathbf{H}^{[k]\mathsf{H}}(\mathbf{R}_{\tilde{\mathbf{z}}} + \tilde{p}\beta M\mathbf{I})^{-1}\right|. \tag{22}$$

Letting the SNR level $P \to \infty$, while keeping the SIR fixed, the achievable rate expression converges to

$$R_{\rm A} = \frac{K}{M+K-1}\mathbb{E}\log\left|\mathbf{I} + \frac{1}{\beta M}\mathbf{H}^{[k]}\mathbf{H}^{[k]\mathsf{H}}\right|. \tag{23}$$

[2]Achievability of (18) can be established by using a long code over many BIA super-symbols, and scrambling the codeword symbols, such that eventually the decoder sees the interference as independent from symbol to symbol (after de-interleaving). Then, the conditioning on $\mathbf{H}_{\rm I}$ in the covariance of interference disappears.

As (23) reveals, at this interference-limited extreme, the achievable rate reduces to $\frac{K}{M+K-1}$ times the capacity of a conventional $M \times M$ SU-MIMO channel with SNR $= -10\log_{10}\beta$ dB.

B. Scenario B: Synchronous Non Aligned Code Reuse

In Scenario B, the interference signal $\mathbf{x}_{\rm I}(n)$ is another BIA code transmitted by the neighboring base station. This BIA code uses the same (M, K) and δ to transmit information streams to the K users in a neighboring cell. However, unlike Scenario A, the two BIA codes are *not* aligned.

We first consider the case $M = 2$ with arbitrary but fixed K. We restrict our attention to the BIA code structure presented in [3], and consider re-orderings of the slots in the BIA code structure in the neighboring cell. We note that mis-alignment of the two BIA codes in the $(M = 2,\ K \geq 2)$ case is equivalent to having the two base stations (i.e., anchor and interfering BSs) transmit their "sum-of-user-symbols" sample (one-slot alignment block 1) on *different* slots. Given that $\mathbf{x}(n)$ has the structure (7) and uses slot 1 to transmit its alignment block 1, a mis-aligned BIA transmission arises by having the interfering cell transmit its alignment block 1 in one of the K slots following the first one. All K such choices are equivalent from the point of view of ergodic rate performance. Thus, without loss of generality, we assume $\mathbf{x}_{\rm I}(n)$ is given by[3]

$$\mathbf{x}_{\rm I}(1) = \mathbf{u}_{\rm I}^{[K]} \tag{24a}$$

$$\mathbf{x}_{\rm I}(n) = \mathbf{u}_{\rm I}^{[n-1]} \qquad \text{for } 2 \leq n \leq K \tag{24b}$$

$$\mathbf{x}_{\rm I}(K+1) = \sqrt{\delta}\textstyle\sum_{k=1}^{K}\mathbf{u}_{\rm I}^{[k]}. \tag{24c}$$

Following again the zero-forcing post-processing step (8), and using (7) and (24) in the receive model (16), yields at user k the following post-processed measurements

$$\tilde{\mathbf{y}}^{[k]} = \mathbf{H}^{[k]}\mathbf{u}^{[k]} + \sqrt{\beta}\overline{\mathbf{H}}_{\rm I}^{[k]}\mathbf{u}_{\rm I} + \tilde{\mathbf{z}}^{[k]} \tag{25}$$

where $\tilde{\mathbf{z}}^{[k]} \sim \mathcal{CN}(\mathbf{0}, \mathbf{R}_{\tilde{\mathbf{z}}})$, with $\mathbf{R}_{\tilde{\mathbf{z}}}$ given by (9),

$$\mathbf{u}_{\rm I} = \begin{bmatrix}\mathbf{u}_{\rm I}^{[1]\mathsf{T}} & \mathbf{u}_{\rm I}^{[2]\mathsf{T}} & \cdots & \mathbf{u}_{\rm I}^{[K]\mathsf{T}}\end{bmatrix}^{\mathsf{T}}$$

and $\overline{\mathbf{H}}_{\rm I}^{[k]}$ can be expressed in the following form

$$\overline{\mathbf{H}}_{\rm I}^{[k]} = \begin{bmatrix}\mathbf{h}_{\rm I}^{[k]}(1) & \mathbf{0} \\ \mathbf{0} & \mathbf{h}_{\rm I}^{[k]}(2)\end{bmatrix}\mathbf{B}_{\rm I}^{[k]}, \tag{26}$$

and where the $4 \times 2K$ matrix $\mathbf{B}_{\rm I}^{[k]}$ is user specific. Without loss of generality we focus on the rates provided to users 1 and K. The rate provided to user k for any $1 < k < K$ is the same as the rate provided to user 1. For user 1, we have

$$\mathbf{B}_{\rm I}^{[1]} = \begin{bmatrix}-\sqrt{\delta}\mathbf{I} & -(1+\sqrt{\delta})\mathbf{I} & \cdots & -(1+\sqrt{\delta})\mathbf{I} & \frac{1-\delta}{\sqrt{\delta}}\mathbf{I} \\ \mathbf{I} & \mathbf{0} & \cdots & \mathbf{0} & \mathbf{0}\end{bmatrix} \tag{27}$$

while for user K

$$\mathbf{B}_{\rm I}^{[K]} = \begin{bmatrix}-\mathbf{I} & -\mathbf{I} & \cdots & -\mathbf{I} & \frac{1}{\sqrt{\delta}}\mathbf{I} \\ \sqrt{\delta}\mathbf{I} & \sqrt{\delta}\mathbf{I} & \cdots & \sqrt{\delta}\mathbf{I} & \sqrt{\delta}\mathbf{I}\end{bmatrix}. \tag{28}$$

[3]Note that asynchronous operation of a common BIA code structure can be captured by a minor modification of (24) and the subsequent analysis.

Assuming that the instantaneous covariance of the interference signal is unknown to the kth receiver, the sum-achievable rate in the cell of interest is given by:

$$R_{\mathrm{B}} = \sum_{k=1}^{K} R_{\mathrm{B}}^{[k]} = (K-1)R_{\mathrm{B}}^{[1]} + R_{\mathrm{B}}^{[K]} \tag{29}$$

where $R_{\mathrm{B}}^{[k]}$ is the achievable rate of user k in the cell of interest, and is given by:

$$R_{\mathrm{B}}^{[k]} = \frac{1}{K+1}\mathbb{E}\log\left|\mathbf{I} + \tilde{p}\mathbf{H}^{[k]}\mathbf{H}^{[k]^{\mathsf{H}}}\left(\overline{\mathbf{R}}_{\mathbf{v},\mathrm{B}}^{[k]}\right)^{-1}\right| \tag{30}$$

with

$$\overline{\mathbf{R}}_{\mathbf{v},\mathrm{B}}^{[k]} = \mathbf{R}_{\tilde{\mathbf{z}}} + \tilde{p}\beta\overline{\mathbf{R}}_{\mathrm{I,B}}^{[k]} \tag{31}$$

and

$$\overline{\mathbf{R}}_{\mathrm{I,B}}^{[k]} = \begin{cases} 2\mathrm{diag}(K-4+K\delta+2(K-2)\sqrt{\delta}+\delta^{-1},\ 1) & \text{if } k < K \\ 2\mathrm{diag}\left(\delta^{-1}+K-1,\ K\delta\right) & \text{if } k = K \end{cases}. \tag{32}$$

For an (M, K) code with $M > 2$, and a specific permutation of the BIA code structure in the neighboring cell, a similar ergodic-rate analysis can be carried out. Similarly, to the $M = 2$ case, the rates are given in the form (30), where the interference covariances, $\overline{\mathbf{R}}_{\mathbf{v},\mathrm{B}}^{[k]}$, are permutation and user specific. Here, however, we only focus on the case $M = 2$ for Scenario B, since the number of possible permutations, grows exponentially fast with increasing M and K and is prohibitively large even with $M = 3$ and $K = 2$.

C. Scenario C: White Isotropic Interference

Under Scenario C, $\mathbf{x}_{\mathrm{I}}(1), \mathbf{x}_{\mathrm{I}}(2), \cdots, \mathbf{x}_{\mathrm{I}}(K+1)$ are mutually independent zero-mean vectors with covariance equal to a scaled identity matrix. This case can model a number of interference scenarios, including the following:

- The interference is a sample-interleaved BIA transmission; $\mathbf{x}_{\mathbf{I}}(n)$ is generated as the output of an interleaver with input the sequence of BIA codewords intended for the users in the interfering cell.
- The interfering sequence models the sum of one or more uncoordinated interfering transmissions with, e.g., as from conventional MU-MIMO or SU-MIMO.

We focus on the constant interference power case[4].

For any fixed but arbitrary power-ratio, δ, used in the BIA scheme for $\mathbf{x}(n)$, the sum-achievable rate for the anchor cell is given by the associated isolated-cell expression in Theorem 2 with SNR replaced by SINR. Hence, the sum-achievable rate under scenario C can be expressed as follows

$$R_{\mathrm{C}} = \frac{K}{M+K-1}\mathbb{E}\log\left|\mathbf{I} + \frac{\tilde{p}}{1+P\beta}\mathbf{H}^{[k]}\mathbf{H}^{[k]^{\mathsf{H}}}\mathbf{R}_{\tilde{\mathbf{z}}}^{-1}\right|. \tag{33}$$

Letting again SNR $\to \infty$, while keeping the SIR $= 1/\beta$ fixed, for the constant power BIA ($\delta = 1/K$) we obtain

$$R_{\mathrm{C}} = \frac{K}{M+K-1}\mathbb{E}\log\left|\mathbf{I} + \frac{1}{\beta M}\mathbf{H}^{[k]}\mathbf{H}^{[k]^{\mathsf{H}}}\mathbf{R}_{\tilde{\mathbf{z}}}^{-1}\right|. \tag{34}$$

[4]In the cases corresponding to non-constant power BIA transmission, the interference power varies over slots. These cases can be worked out similarly the constant-power interference scenario considered here and show similar performance trends.

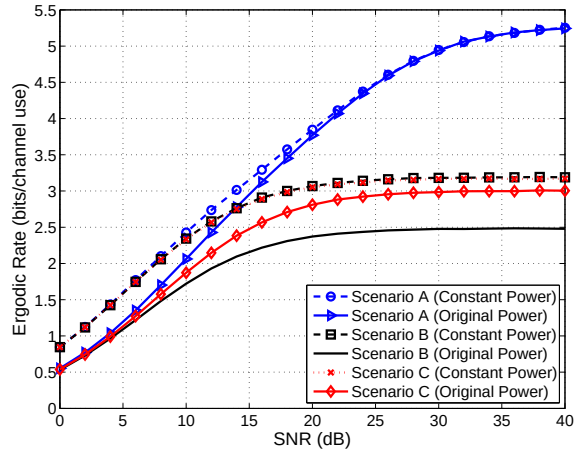

Fig. 5. Ergodic Rate vs. SNR for $(M, K) = (2, 20)$ and SIR $= 10$ dB.

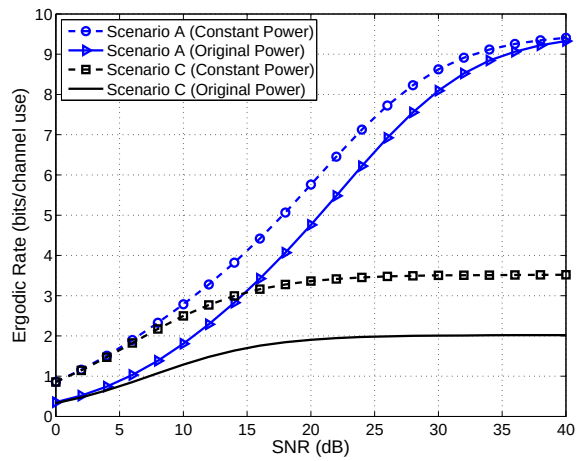

Fig. 6. Ergodic Rate vs. SNR under Scenarios A and C, when $(M, K) = (4, 20)$ and SIR $= 10$ dB

D. Performance Comparisons

In this section we consider a performance comparison of the three ICI scenarios A, B, and C. Simple inspection of the ergodic-rate of the constant-power BIA scheme under each scenario suggests that BIA yields the best performance under Scenario A. In comparing the ergodic rates provided under Scenarios A and C, it is convenient to re-express the ergodic rate (33) under scenario C, in the form (18), with $\overline{\mathbf{R}}_{\mathbf{v},\mathrm{A}}$ replaced by $\overline{\mathbf{R}}_{\mathbf{v},\mathrm{C}} = \mathbf{R}_{\tilde{\mathbf{z}}} + \tilde{p}\beta\mathbf{R}_{\mathrm{I,C}}^{[k]}$, and where

$$\overline{\mathbf{R}}_{\mathrm{I,C}} = M\mathbf{R}_{\tilde{\mathbf{z}}}\ . \tag{35}$$

Since $\mathbf{R}_{\mathrm{I,C}} - \mathbf{R}_{\mathrm{I,A}}$ is positive semi-definite, the achievable rate given in (23) is higher than that in (34), especially with large K and high interference levels. Similarly, the ergodic rate (23) under Scenario A is higher than the one provided in scenario B, as $\mathbf{R}_{\mathrm{I,B}}^{[k]} - \mathbf{R}_{\mathrm{I,A}}$ for all k is again positive semi-definite.

The following figures present a comparative study of the ergodic rates under the three ICI scenarios. Figs. 5 and 6 show the ergodic rate performance of the BIA scheme in the cell of interest, as a function of SNR, at SIR equal to 10 dB.

As Fig. 5 shows, the rate provided by a fixed-δ BIA scheme under Scenario A is uniformly higher than the rates under the other two ICI scenarios. In the limit of SNR $\to \infty$, where

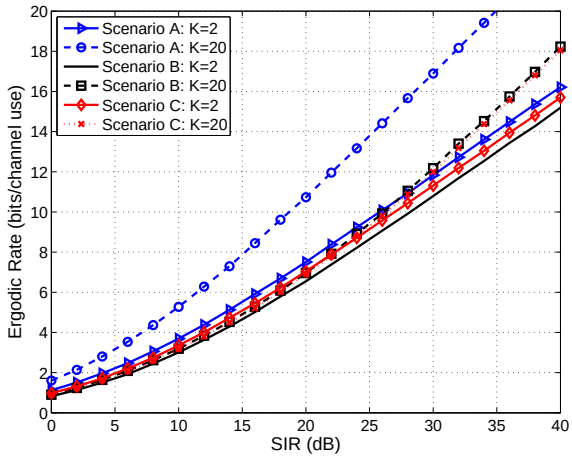

Fig. 7. Ergodic Rates of constant-power BIA vs. SIR (with SNR $\to \infty$) in two-cell setting under Scenarios A, B and C, with $M = 2$ and $K = 2$, 20.

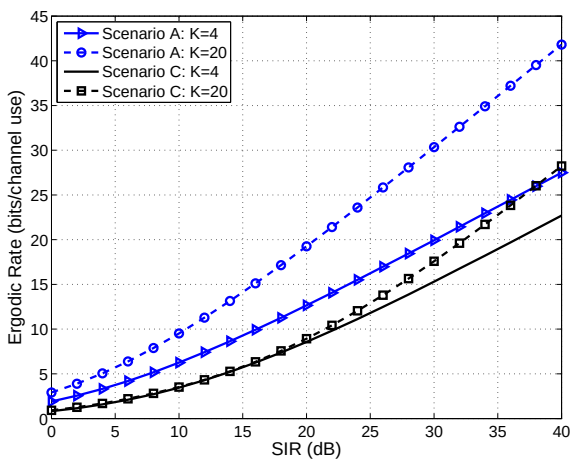

Fig. 8. Ergodic Rates of constant-power BIA vs. SIR (with SNR $\to \infty$) in two-cell setting under Scenarios A, and C, with $M = 4$ and $K = 4$, 20.

the system becomes interference limited, power allocation in the BIA scheme is helpful in increasing the ergodic rates only under Scenarios B and C. In contrast, under Scenario A, as SNR $\to \infty$, power allocation becomes secondary, since the ergodic BIA rate approaches (23), regardless of the δ value.

The case depicted in Fig. 6 has the same number of users as in Fig. 5 but the number of transmit antennas (and receive antenna modes) are increased from $M = 2$ to $M = 4$. Comparisons of the Figs. 5 and 6 suggests that when M is increased from $M = 2$ to $M = 4$, significant rate increases are realized under Scenario A, but not under Scenario C.

Fig. 7 shows the high-SNR ergodic rate performance of the BIA scheme in the cell of interest, as a function of SIR, under the three intercell interference scenarios of interest in the case $M = 2$. As the figure reveals, for each value of K the BIA performance is best under Scenario A (aligned BIA intercell interference). Although increasing the number of users from $K = 2$ to $K = 20$ yields a DoF increase from $MK/(M + K - 1)$ = 4/3 to 40/21, such DoF improvement *does not* necessarily translate to increased rates.

In particular, at low and moderate SIRs, the increased multiplexing gains by switching from a $K = 2$ to a $K = 20$

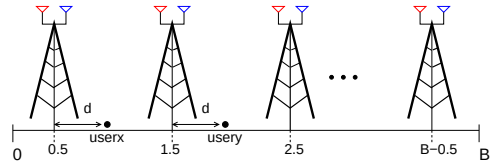

Fig. 9. Cell-based Network

scheme, translate to increased rates *only* under Scenario A. As the figure suggests, aligning the BIA code structure across cells would be vital in realizing high-cell edge rates. Fig. 8 considers the $M = 4$ case and provides further justification for an aligned BIA code structure. At e.g., 10 dB SIR, going from $K = 4$ (DoF = 16/7) to $K = 20$ (DoF = 80/23), yields no rate improvements under scenario C, but significant ones under scenario A.

Note that under Scenarios A and B, the ergodic rates provided to the users can be improved if the instantaneous covariance of the interference signal (i.e, $\mathbf{R}_{\mathrm{I,A}}^{[k]}$ and $\mathbf{R}_{\mathrm{I,B}}^{[k]}$, respectively) is known at the kth receiver. For scenario A, the ergodic rates are given in that case by replacing $\overline{\mathbf{R}}_{\mathbf{v},\mathrm{A}}$ in the rate expression (18) with $\mathbf{R}_{\mathbf{v},\mathrm{A}}^{[k]}$ from (19). Similarly for Scenario B, the ergodic rate of the kth user is given by replacing $\overline{\mathbf{R}}_{\mathbf{v},\mathrm{B}}^{[k]}$ in the rate expression (30) with

$$\mathbf{R}_{\mathbf{v},\mathrm{B}}^{[k]} = \mathbf{R}_{\tilde{\mathbf{z}}} + \tilde{p}\beta\overline{\mathbf{H}}_{\mathrm{I}}^{[k]}\overline{\mathbf{H}}_{\mathrm{I}}^{[k]^{\mathsf{H}}}.$$

Note, however, that unlike Scenario A, whereby knowing $\mathbf{H}_{\mathrm{I}}\mathbf{H}_{\mathrm{I}}^{\mathsf{H}}$ suffices in determining $\mathbf{R}_{\mathbf{v},\mathrm{A}}^{[k]}$, knowing $\mathbf{R}_{\mathbf{v},\mathrm{B}}^{[k]}$ under Scenario B also requires knowing the misalignment pattern.

IV. Cellular using Aligned BIA Code Structures

The two-cell analysis of the Section III motivates the use of a synchronous aligned BIA code structure across an extended cellular topology. For simplicity we focus on the performance of such structures in a 1D wrapped cellular model as shown in Figure 9 [2].

The topology is normalized to an interval $[0, B)$, with $B = 8$ cells and cell b spanning the region $[b, b+1)$ for $b = 0, \ldots, 7$. In cell b, there is one N_t-antenna BS located at $b + 0.5$. In order to eliminate boundary effects, we assume a wrapped topology so that the distance between points x_1, $x_2 \in [0, B)$ in the wrapped topology distance is the minimum of $|x_1 - x_2|$ and $B - |x_1 - x_2|$. We assume a path loss model of form

$$g(d) = G_0 s^{\kappa}/(s^{\kappa} + d^{\kappa}) \tag{36}$$

where $d > 0$ is the distance between the user and its anchor BS, κ is the propagation exponent, and s is the 3 dB breakpoint distance [2]. The constant G_0 sets the transmit power at each BS and implicitly the received SNR. For the transmission in each slot in each cell, we assume that constant power transmission is employed.

A. Code-Reuse and Frequency-Reuse in Aligned BIA

We first consider some interesting deployment options of aligned BIA code structures. We will illustrate such aspects in systems where transmission resources are divided into time

TABLE I

CODE AND POWER ASSIGNMENTS OVER ALL BANDS USING CODE-REUSE 1

Alignment code index k \ Base-station index b	b=1	b=2	b=3	b=4	b=5	•••	b=B
k=1	P_s	P_s	P_s	P_s	P_s	•••	P_s
⋮	⋮	⋮	⋮	⋮	⋮	•••	P_s
k=K	P_s	P_s	P_s	P_s	P_s	•••	P_s

TABLE II

CODE AND POWER ASSIGNMENTS OVER ALL BANDS USING CODE REUSE 2

Alignment code index k \ Base-station index b	b=1	b=2	b=3	b=4	b=5	•••	b=B
k=1,3,5,...	$2P_s$	0	$2P_s$	0	$2P_s$	•••	0
k=2,4,6,...	0	$2P_s$	0	$2P_s$	0	•••	$2P_s$

"slots" and/or frequency "bands", as in an OFDM system. However, it should be clear that similar concepts can apply in other systems with orthogonal resources split in other ways.

In a given resource, e.g. frequency band, a single (M, K) code-structure (with $M \leq N_t$) operates across the cellular deployment. We assume that every active cell on a band operates the same (M, K) BIA code structure synchronously with all the other cells (say within the cyclic prefix constraints of an OFDM design), and each user performs the required alignment operation with respect to this (M, K) structure. Thus the kth BIA-code is aligned across the cellular topology (for $k = 1, \cdots, K$) as in the 2-cell model of Scenario A.

The result of the aligned operation is that, after zero-forcing intra-cell interference in its receiver, a user obtains effectively a $M \times M$ SU-MIMO channel as in (5). With the aligned system, transmissions from all cells using different BIA-codes (different k) do not interfere. However transmissions from different cells using the same code k do interfere. The system can therefore be modeled effectively as a system divided into K available decoupled MU-SU-MIMO (interference) channels in each cell, one per BIA code indexed by $k = 1, 2, \cdots, K$.

This viewpoint offered by the Aligned BIA Code Structure allows for very flexible user scheduling and system operation. To illustrate, consider the case shown in Table I whereby all the codes are used within each cell on all bands, and all user streams are allocated equal transmit power P_s. This corresponds to a code-reuse 1 frequency-reuse 1 scenario.

Table II describes a system that assigns a given code in

TABLE III

FREQUENCY REUSE 2 WITH CODE-REUSE 1

Band index f, code index k \ Base-station index b	b=1	b=2	b=3	b=4	b=5	•••	b=B
f=1, k=1,2,3,... (all k)	$2P_s$	0	$2P_s$	0	$2P_s$	•••	0
f=2, k=1,2,3,... (all k)	0	$2P_s$	0	$2P_s$	0	•••	$2P_s$

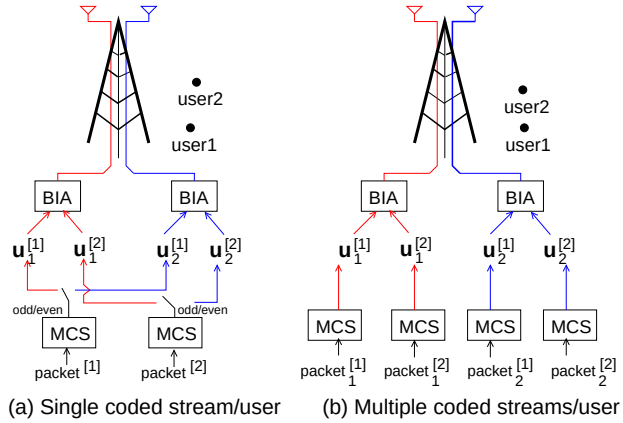

Fig. 10. Two deployments of cellular with $(M, K) = (2, 2)$ and $N_t = 2$

a regular fashion once every two cells, with each cell using only half of the codes on each band. The power assigned to each code is the same. This corresponds to a code-reuse 2 frequency-reuse 1 case. Note that powers in Table II are doubled compared to Table I so that the average transmit power per band within each cell is the same in both cases.

Table III shows a conventional frequency reuse 2 system whereby all the codes are used for transmission by a base-station on its active bands. Interestingly, if users operating under Table II perform the same alignment operations with respect to all K codes the performance of the schemes in Tables II and III are equivalent. This can be understood by noting that the interference on any given code in both systems is the same, i.e. coming from every other station with all such stations using transmission power $2P_s$ on each code.

B. Operation of Aligned BIA in Cells and Clusters

BIA has some interesting deployment options and operational aspects when applied to cellular. Fig. 10 illustrates two possible deployments of cellular using $(M, K) = (2, 2)$ and code-reuse 1. In the figure "$\mathsf{packet}_i^{[k]}$" refers to the ith uncoded data packet for user k, MCS the modulation/coding scheme used, and BIA the arithmetic operations required to correctly combine coded symbols for transmission. In Fig. 10(a) each user has a single data packet producing a single coded stream. Half the coded symbols (e.g. odd symbols) are used for transmissions on one antenna, and the other symbols (e.g. even symbols) are used for the other antenna.

In Fig. 10(b) each user has two data-packets each producing their own coded stream. One coded stream drives one antenna, and the other coded stream the other. Interesting, in terms of ergodic rates, whereby the coded stream(s) for any user span transmissions across many channel realizations (e.g. many $\mathbf{H}^{[k]}$ in (5)), the performance of the two systems is equivalent. Approximations to such an operation can happen in practice, for example, if coded symbols are applied to different independently fading tones in an OFDM system.

Fig. 10(b) has a natural extension to operations across clusters as shown in Fig. 11. Here one simply splits the antennas of one cell between two cells so that each station now has a single antenna ($N_t = 1$). The example illustrates one

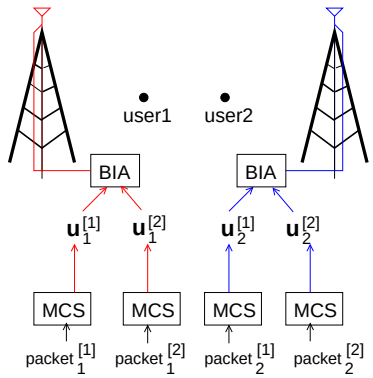

Fig. 11. A cluster with code-reuse 1, $(M, K) = (2, 2)$, and $N_t = 1$

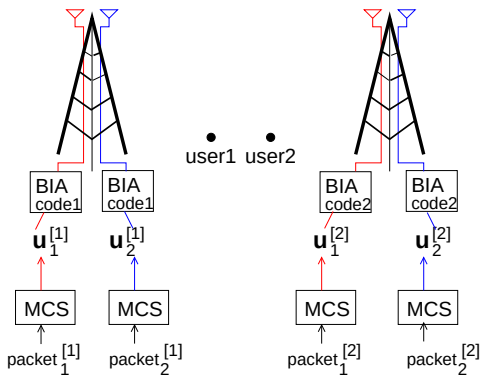

Fig. 12. Cellular with code-reuse 2, $(M, K) = (2, 2)$, and $N_t = 2$

operational benefit of BIA when applied to clusters. Specifically, each station (antenna) can operate using independent data packets and independent coded streams. This is unlike the application of traditional MU-MIMO techniques, such as LZFB, to clusters as often done in a Network MIMO [2]. For LZFB common coded streams have to be shared between stations in order to apply the necessary precoding determined by beamforming vectors. Furthermore, and interestingly, under some conditions accounting for CSIR and CSIT overheads, BIA can in fact outperform LZFB in cluster operations [5].

One can take the case of Fig. 11, rearrange packets and BIA-codes so that each station only serves one user on one code. This is a cellular scheme with code-reuse 2 with $N_t = 2$ as in Fig. 12. An interesting comparison can be made between Fig. 11 and Fig. 12 for users equidistant between the two stations. For such users, assuming the same pathloss and statistically equivalent channels to each station, the performance of both systems is equivalent. However, as users move away from cluster centers and experience stronger channels to one of the two stations, exploiting this stronger channel via a cellular scheme, or by power allocations to streams, can be beneficial.

Finally, a subtle point to make concerns the number of antenna modes required by different systems. All users in all schemes of Fig. 10 to Fig. 12 require only $M = 2$ antenna modes. Thus, from the point of view of user hardware, such schemes are roughly comparable. However, the cluster scheme uses $N_t = 1$ while cellular $N_t = 2$. In order for the cluster scheme to make full use of $N_t = 2$ one would have to consider more antenna modes at the user using schemes (M, K) with $M = 4$. Thus, BIA brings in another dimension in user hardware that must be considered in addition to station hardware when comparing schemes.

V. Performance of Aligned BIA with Code Reuse F

A. Ergodic Rates

Consider, as in Fig. 9, users at location d in cell with $d \in [0, 1/2)$ and a band using code-reuse F. Assume that for each cell K/F such users are served simultaneously by a cell, each user being assigned one of the codes $k = 1, \ldots, K/F$. Building upon the equivalence of the schemes in Tables II and III we will determine the long-term ergodic rate provided at the user location d by the cellular with code-reuse 1 and conventional frequency-reuse F simultaneously serving K users at location d [5].

Without loss in generality, consider cell $b = 0$ and an arbitrary code k. Let $\mathbf{u}_b$ denote the information stream transmitted by BS b on the code (for simplicity we omit the dependence of all variables on the index k), and $\mathbf{H}_b$ denote the $M \times M$ matrix with i^{th} row denoting the vector channel between the M transmit antennas of base station b and the ith antenna mode of the receiver using the kth code in cell 0. The effective (post intra-cell interference cancellation) SU-MIMO channel for the given user at cell 0 is given by

$$\mathbf{y} = \sqrt{g(d)}\sqrt{F}\mathbf{H}_0\mathbf{u}_0 + \tilde{\mathbf{z}} + \sqrt{F}\sum_{b=1}^{B/F}\sqrt{g(|bF-d|)}\mathbf{H}_{bF}\mathbf{u}_{bF}$$

whereby $\mathbb{E}[\mathbf{u}_{mF}\mathbf{u}_{mF}^{\mathsf{H}}] = 1/M$, the $(i,j)^{th}$ entry of the $N_t \times N_t$ matrix $\mathbf{H}_{mF}$ denotes the channel between cell j TX antenna of BS m and the ith receive antenna mode of the user terminal, and where $\tilde{\mathbf{z}} \sim \mathcal{CN}(0, \mathbf{R}_{\tilde{\mathbf{z}}})$ is the noise covariance after ZF intracell interference and is given by (11).

For convenience, let

$$\mathbf{v} = \tilde{\mathbf{z}} + \sqrt{F}\textstyle\sum_{b=1}^{B/F}\sqrt{g(|bF-d|)}\mathbf{H}_{bF}\mathbf{u}_{bF}$$

denote the aggregate interference vector plus noise experienced at the user receiver after ZF alignment. In the case that the covariance matrix $\mathbf{R}_{\mathbf{v}}$ is known (i.e., has been estimated) at the user location, the following rate is achievable serving K/F users at location d:

$$\bar{R}^{\text{BIA}}(d; M, K) = \tfrac{K/F}{M+K-1}\mathbb{E}\log\left|\mathbf{I} + \frac{F\,g(d)}{M}\mathbf{H}_0\mathbf{H}_0^{\mathsf{H}}\mathbf{R}_{\mathbf{v}}^{-1}\right|$$

where $\mathbf{R}_{\mathbf{v}} = \mathbf{R}_{\tilde{\mathbf{z}}} + \sum_{b=1}^{B/F}\frac{F\,g(|bF-d|)}{M}\mathbf{H}_{bF}\mathbf{H}_{bF}^{\mathsf{H}}$ and $\mathbf{R}_{\tilde{\mathbf{z}}}$ is given by (11).

In the case that the intercell interference covariance $\mathbf{R}_{\mathbf{v}}$ is unknown at the user location the following rate is achievable serving K/F users at location d using mismatched decoding.

$$\bar{R}^{\text{BIA}}(d; M, K) = \tfrac{K/F}{M+K-1}\mathbb{E}\log\left|\mathbf{I} + \frac{F\,g(d)}{M}\mathbf{H}_0\mathbf{H}_0^{\mathsf{H}}\bar{\mathbf{R}}_{\mathbf{v}}^{-1}\right|$$

[5]Note that in practice the K users can be randomly distributed over the range of each cell. Such analysis is beyond the scope of this paper.

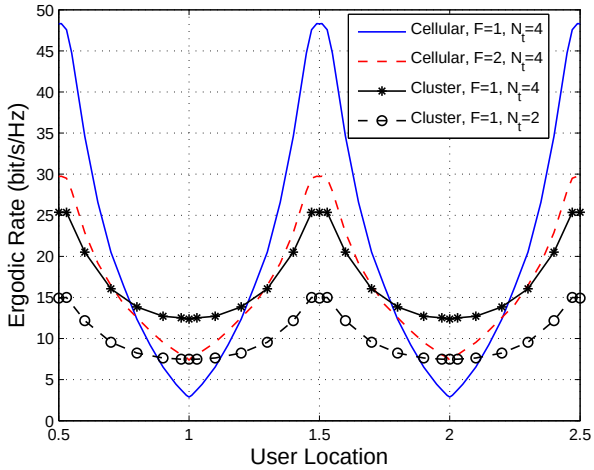

Fig. 13. Performance of Cellular with $F = 1$ and $F = 2$ and where $(M, K) = (N_t, 20)$ for cellular and $(M, K) = (2N_t, 20)$ for clusters, $G_0 = 70$ dB and $\kappa = 3.8$

where $\bar{\mathbf{R}}_{\mathbf{v}} = \mathbb{E}\mathbf{R}_v = \mathbf{R}_{\tilde{\mathbf{z}}} + F\mathbf{I}\sum_{b=1}^{B/F} g(|bF - d|)$ and $\mathbf{R}_{\tilde{\mathbf{z}}}$ is given by (11).

For clusters we consider system whereby alternating pairs of clusters operate on the same band. That is, given two bands and $B = 8$, clusters of stations $[0, 1]$, $[2, 3]$, $[4, 5]$, $[6, 7]$ operate synchronously on one band serving users a distance $d \in [0, 1]$ from the left station, and clusters of stations $[1, 2]$, $[3, 4]$, $[5, 6]$, $[7, 0]$ operate synchronously on the other band serving users a distance $d \in [0, 1]$ from the left station. Noting the similarities between Fig. 10(b) to Fig. 12, similar ergodic rate expressions can be derived noting the differences in pathloss between different stations in and between clusters.

B. Examples

We evaluate the ergodic rates of different systems via Monte Carlo simulations of the various rate expressions previously described. In Fig. 13 we one considers the effect of code reuse and cluster operation as a function of the user location d. For each location the common $(M, K = 20)$ BIA scheme is used. The value of M is chosen as $M = N_t$ for cellular and $M = 2N_t$ for cluster operation. For the pathloss described in (36) values $G_0 = 10^7$, $s = 0.05$ and $\kappa = 3.8$ are used.

Comparing the cellular schemes one can see the expected benefit of code-reuse (equivalent given our system assumptions to frequency reuse) on cell-edge users. This comes at the classic price to rates of cell-center users. The cluster operation is interesting. To compare clusters to cellular assuming the same number of user antenna modes $M = N_t = 4$, the clusters operate with $N_t = 2$ antennas per station. As shown in the figure, and noted previously, cluster-center users have the same performance as cell-edge users in the cellular code-reuse 2 case. Furthermore, with equal-power allocation to streams clusters begin to lose with respect to cellular for users that have increased pathloss from one of the stations (users away from the cluster center). However, a cluster scenario with $N_t = 4$ operating a BIA scheme with respect to the code for (M, K) where $M = 8$ does have benefits over cellular for a range of users away from the cluster-center. This is due to the reduction in inter-cell (inter-cluster) interference provided by cluster transmission. However, to exploit this users must now have up to $M = 2N_t = 8$ antenna modes.

VI. Conclusion

Blind interference alignment (BIA) MU-MIMO schemes [3] are of interest, due to their ability to increase DoFs with reduced CSIT overheads. To realize these DoF gains, BIA MU-MIMO has to rely on user terminals with the ability to switch fast among multiple receive-antenna modes.

In this work we consider the use of BIA MU-MIMO schemes in cellular and cluster architectures. As we show, using a common aligned BIA code structure across the deployment has many performance and operational advantages. Using a two-cell example we show that an aligned BIA code structure uniformly outperforms interleaved and non-aligned BIA code structures, as it allows receivers to align and eliminate a significant portion of their inter-cell interference.

Operationally, an aligned BIA code structure allows for flexible operations across cells using both traditional frequency-reuse and alignment code-reuse (which can be equivalent for some, but not all, cases). Such aligned structures enable high cell-edge throughout performance with either frequency (or code) reuse in cellular, or cluster transmission. BIA also allows a simplified operation for cluster systems as it works independently of CSIT and readily allows each station in a cluster to transmit independent information streams. However, cluster operation may also require users to support more antenna modes, and thus BIA does have user hardware implications different from those in traditional CSIT-based MU-MIMO.

Several issues require further study to evaluate the potential of BIA MU-MIMO in cellular and beyond. These include performance under more realistic channel models, as well as accounting for training in performance and overheads [5]. Advances in BIA MU-MIMO schemes are also are needed in order to reduce the BIA codeword lengths, which, for large M and K values, can be exceedingly large [3].

References

[1] G. Caire, N. Jindal, M. Kobayashi, and N. Ravindran, "Multiuser MIMO achievable rates with downlink training and channel state feedback," *IEEE Trans. on Inform. Theory*, vol. 50, no. 6, July 2010.

[2] S. Ramprashad, G. Caire, and H. Papadopoulos, "Cellular and Network MIMO Architectures: MU-MIMO Spectral Efficiency and Costs of Channel State Information," in *Proc. IEEE Asilomar Conf. Sig., Sys, Computers*, pp. 1811-1818, Nov. 2009.

[3] C. Wang, T. Gou and S. Jafar, "Aiming Perfectly in the Dark - Blind Interference Alignment through Staggered Antenna Switching", *http://arxiv.org/abs/1002.2720*, Feb. 2010.

[4] G. Caire, S. A. Ramprashad, H. C. Papadopoulos, C. Pepin, and C.-E. W. Sundberg, "Multiuser MIMO downlink with limited inter-cell cooperation: Approximate interference alignment in time, frequency and space," in *Proc. 46th Allerton Conf. Commun., Control and Computing*, pp. 730–737, Oct. 2008.

[5] C. Wang, H. C. Papadopoulos, S. A. Ramprashad and G. Caire, "Improved Blind Interference Alignment in a Cellular Environment using Power Allocation and Cell-Based Clusters", in *Proc. ICC*, June 2011, Kyoto, Japan.